# Relationship between $SiO_2$ content and electrical properties of 8-mol% $Y_2O_3$-stabilized $ZrO_2$ electrolyte

Susumu Nakayama (Depart. of Applied Chemistry and Biotechnology, National Institute of Technology (KOSEN), Niihama College, s.nakayama@niihama-nct.ac.jp, Japan)
Kazunari Itani (Advanced Engineering Course, KOSEN, Niihama College, c1400002@niihama.kosen-ac.jp, Japan)
Tadashi Yasui (Daiichi Kigenso Kagaku Kogyo Co., Ltd., t_yasui@dkkk.co.jp, Japan)
Satoshi Watanabe (Daiichi Kigenso Kagaku Kogyo Co., Ltd., s_watanabe@dkkk.co.jp, Japan)
Takao Mizuno (Daiichi Kigenso Kagaku Kogyo Co., Ltd., t_mizuno@dkkk.co.jp, Japan)

## Abstract

After preparing 8-mol% $Y_2O_3$-stabilized $ZrO_2$ electrolytes with $SiO_2$ contents to < 40, 550, 1200, and 2800 ppm and attaching Pt electrodes, a direct-current (DC) load test wherein 1 V was applied at 800 °C in air atmosphere for 1000 h was conducted to investigate the effect of $SiO_2$ on the electrical properties. The DC resistance at 800 °C for all samples increased immediately after the test was started, but tended to stabilize over time, and remained almost constant after approximately 600 h. The bulk and the grain-boundary resistances measured by the AC complex impedance analysis at 300 °C after the DC voltage load test were increased in all samples compared to that before the test, but no clear correlation was found between the amount of $SiO_2$ and the resistance. Moreover, the electrode interface resistance measured by complex impedance analysis at 800 °C also increased after the DC voltage load test.

## Key words

impedance analyzer, Nyquist plot, 8YSZ, scanning electron microscope, X-ray diffraction

## 1. Introduction

Among the raw materials of yttria-stabilized zirconia (YSZ), an electrolyte material for solid oxide fuel cells (SOFCs) (Tikkanen et al., 2011; Samui et al., 2016; Bouhamed, 2017; Cong et al., 2020), the standard values of certain aspects are determined by SOFC-making companies. These aspects include composition, average particle size, and specific surface area. In addition, the allowable range of the amount of impurities is an important factor. However, there have only been a few studies on the effects of impurities on the electrical properties of electrolytes. In contrast, the electrical resistance of YSZ is known to increase when the material is held at a high temperature for a long time. In addition, the electromotive force of SOFCs using YSZ as an electrolyte decreases when used at high temperatures for a long time. Therefore, it is necessary to elucidate and remedy the cause of this reduction (Ciacchi and Badwal, 1991; Yamamoto et al., 1995; Hattori et al., 2004; Kwon and Choi, 2006). The raw materials of YSZ generally contain silicon dioxide ($SiO_2$) as an impurity, and such impurities affect the increase in grain-boundary resistance. The baddeleyite ($ZrO_2$, the zirconium ore) contains a few percent $SiO_2$, but the $SiO_2$ content can be reduced to 500-3000 ppm by the acid treatment process of impurity removal. In this study, we assumed that the abovementioned increase in resistance for YSZ exposed to high temperatures for a long time was related to the $SiO_2$ impurity in the YSZ (Hughes and Badwal, 1991). Based on this assumption, we investigated the relationship between the amount of $SiO_2$ of < 40 ppm and 500-3000 ppm that is contained in 8-mol% $Y_2O_3$-stabilized $ZrO_2$ (8YSZ) and the changes in the electrical properties.

## 2. Experimental procedure

The 8YSZ raw materials containing $SiO_2$ used in this work were produced by Daiichi Kigenso Kagaku Kogyo Co., Ltd. (Table 1). The raw material was cold isostatic press-molded at 100 MPa and then sintered at 1430 °C. The density of the sintered sample was then measured using the Archimedes method. The sintered sample was processed into a cube with a side length of 5 mm. Pt paste (Tanaka Kikinzoku Kogyo K.K., TR-7905 ($SiO_2$-less type)) was applied to both sides of the sample and baked at 1000 °C to provide a Pt electrode. As

Table 1: Composition (wt.%) of 8YSZ raw materials containing $SiO_2$ used in this work

| | $SiO_2$ content | | | |
|---|---|---|---|---|
| | < 40 ppm | 550 ppm | 1200 ppm | 2800 ppm |
| $SiO_2$ | 0.004 | 0.055 | 0.12 | 0.28 |
| $ZrO_2$ | 86.39 | 86.48 | 86.17 | 86.17 |
| $Y_2O_3$ | 13.61 | 13.52 | 13.83 | 13.83 |
| $Al_2O_3$ | < 0.005 | | | |
| $Fe_2O_3$ | 0.004 | 0.004 | 0.004 | 0.005 |
| $TiO_2$ | 0.001 | 0.002 | 0.001 | 0.002 |
| CaO | 0.002 | 0.001 | 0.001 | 0.001 |
| $Na_2O$ | 0.003 | 0.003 | 0.001 | 0.001 |
| $H_2O$ | 0.17 | 0.31 | 0.38 | 0.33 |
| Ig.loss | 0.35 | 0.58 | 0.34 | 0.41 |

shown in Figure 1, the electrode area and distance between electrodes of the measurement sample were 0.25 $cm^2$ (0.5 cm × 0.5 cm) and 0.5 cm, respectively. The initial electrical properties were measured using an impedance analyser (HP4194A) in the frequency range of 100 kHz to 10 MHz in the atmosphere, and the bulk resistance and the grain-boundary resistance of each sample was determined by complex impedance analysis using an alternating-current (AC) method. After measuring the initial electrical characteristics, the sample was placed in an electric furnace, as shown in Figure 1, and the temperature was raised to 800 °C. A voltage of 1 V was applied across the sample with a regulated direct-current (DC) power supply and maintained.

The voltage load was stopped at regular intervals, the DC resistance was measured using a multimeter (Advantest Co, TR6847) at 800 °C, and the change in DC resistance was monitored for up to 1000 h. After 1000 h of the DC voltage load test, the bulk resistance and the grain-boundary resistance of each sample was determined via complex impedance analysis using the impedance analyzer. After polishing the surface of the sintered sample before and after the DC voltage load test and performing thermal etching treatment, the sample surface was observed using a field-emission scanning electron microscope (JEOL Ltd., JSM-7500F). Furthermore, X-ray diffraction (XRD) data of the # 400 diamond grindstone processed surface of the sintered sample were obtained using an X-ray diffractometer (Rigaku Co., MiniFlex II) with CuKα1 radiation and a graphite monochromator.

## 3. Results and discussion

### 3.1 Initial electrical characteristics

The raw materials used were prepared by setting the $SiO_2$ contents to < 40, 550, 1200, and 2800 ppm while maintaining constant levels of the components other than $SiO_2$. The densities of the sintered samples containing < 40, 550, 1200, and 2800 ppm $SiO_2$ prepared by molding the raw materials and sintering at 1430 °C were 5.77, 5.83, 5.78, and 5.78 $g{\cdot}cm^{-3}$, respectively. As seen in the results, similar densities were obtained for all samples.

In Figure 2, the Nyquist plot for each sample at 300 °C before the DC voltage load test is shown as filled circles. In all samples, arcs originating from the bulk resistance (at the high-frequency side shown on the left section of the figure) and the grain-boundary resistance (at the low-frequency side shown on the right section of the figure) were observed. It is explained in detail in the appendix section. The bulk resistance was almost constant irrespective of the $SiO_2$ content. However, the grain-boundary resistance increased with increasing $SiO_2$ content. This means that $SiO_2$ in the raw material was present at the grain-boundary of 8YSZ and not within

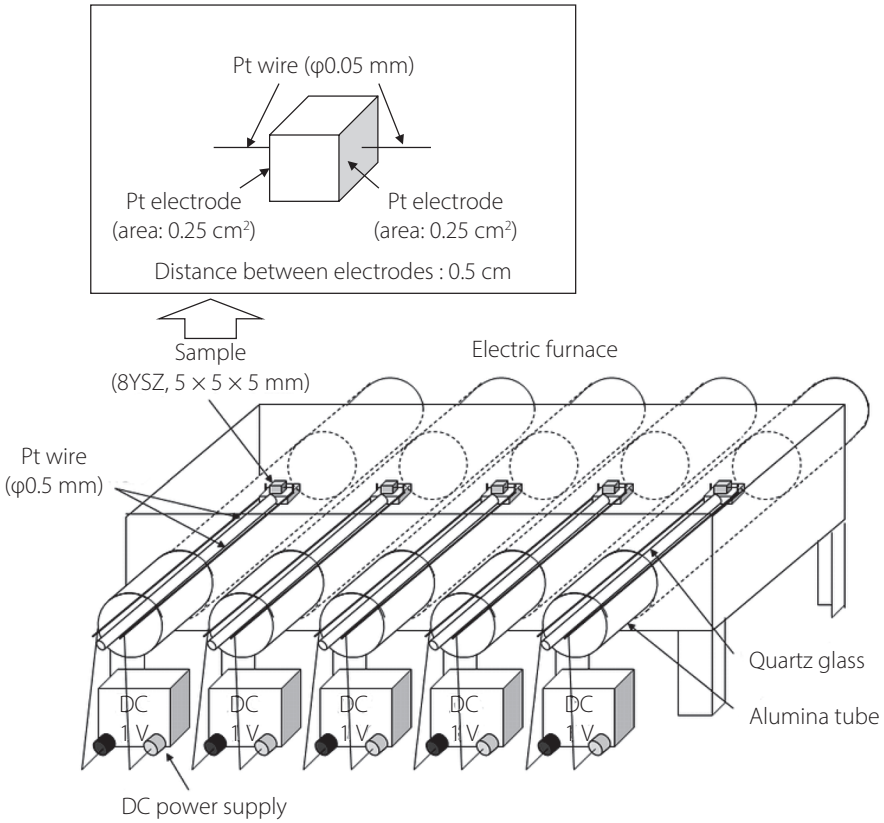


Figure 1: Apparatus for the direct-current (DC) voltage load test for 1000 h at 800 °C and schematic diagram of measurement sample

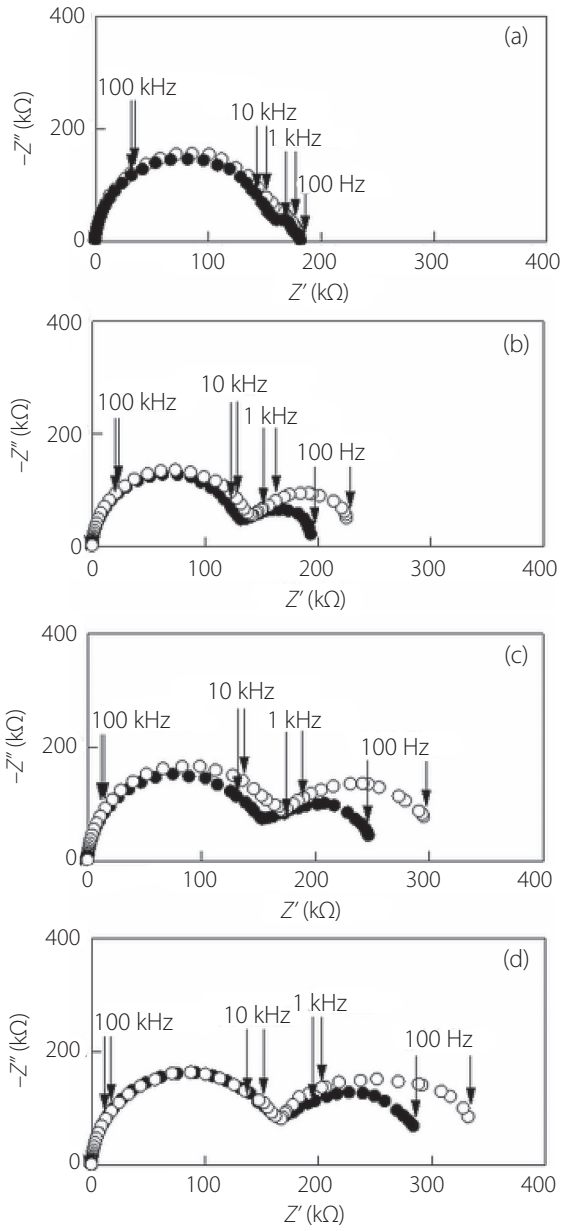


Figure 2: Nyquist plot before (filled circle) and after (open circle) the DC voltage load test of 8YSZ ($SiO_2$ contents: (a) < 40 ppm, (b) 550 ppm, (c) 1200 ppm, and (d) 2800 ppm) at 300 °C

the bulk, and was considered to cause the increase in the grain-boundary resistance. The arc originating from the grain boundary resistance decreased as the temperature increased and could not be observed around 700 °C.

In Figure 3, the Nyquist plot for each sample before the DC voltage load test at 800 °C is shown as filled circles. For all samples, the arcs originating from the bulk and grain-boundary resistances could no longer be observed, only the arc originating from the electrode interface resistance was observed. From the result, the sum of the bulk + grain-boundary resistance is determined by extrapolation to zero reactance of the arc in the higher frequency side. On the other hand, the sum of the bulk + grain-boundary + electrode interface resistance is determined by extrapolation to zero reactance of the arc in the lower frequency side.

### 3.2 DC voltage load test

Figure 4 shows the relationship between the elapsed time and changes in the DC resistance ($R_{dc}$) following the DC voltage load test. In all samples, the DC resistance significantly increased immediately after the test was started, but the increase progressed at a diminished rate as time elapsed. For the samples with high $SiO_2$ contents of 550, 1200, and 2800 ppm, the initial increase in the resistance was large, but the resistance became almost constant after approximately 400 h. In contrast, for the sample with low $SiO_2$ content of < 40 ppm, the resistance increased slowly up to approximately 600 h, and then remained constant. These tendencies were consistent with those reported by Hattori et al. (Hattori et al., 2004).

### 3.3 Electrical properties after the DC voltage load test

In Figure 2, the Nyquist plot at 300 °C after the DC voltage load test is shown as open circles. Figure 5 (a) and (b) show the bulk resistance ($R_b$) and the grain-boundary resistance ($R_{gb}$) at 300 °C, respectively, before and after the test as a function of the $SiO_2$ content, which was obtained via complex impedance analysis. This plot showed that the bulk resistance after the test increased by approximately 5-10 % in all samples. The grain-boundary resistance increased in all samples, but the level of increase was independent of the $SiO_2$ content. Compared with the initial grain-boundary resistance, the grain-boundary resistance after the test increased by 23% for an $SiO_2$ content of < 40 ppm, 28 % for that of 550 ppm, 25 % for that of 1200 ppm, and 26 % for that of 2800 ppm. Therefore, the $SiO_2$ content and the amount of increase in the grain-boundary resistance show little correlation. On the other hand, the bulk resistance after the test was observed to increase slightly (2-10 %) in all samples compared with that before the test.

In Figure 3, the Nyquist plot for each sample after the DC voltage load test at 800 °C is shown as open circles. Figure 5(c) shows the electrode interface resistance ($R_{ei}$) at 800 °C, before and after the test as a function of the $SiO_2$ content. From the plot, the electrode interface resistance after the test was also observed to increase. In addition, the sum ($R_b + R_{gb} + R_{ei}$) of the bulk + grain-boundary resistance and the electrode interface resistance at 800 °C determined from the Nyquist plot in Figure 3 was in agreement with the DC resistance ($R_{dc}$) at 800 °C shown in Figure 4.

The reflected electron images of the thermally etched surfaces of samples with $SiO_2$ contents of < 40 and 2800 ppm before and after the DC voltage load test are shown in Figure 6. The black spots are considered to be pores. A mapping analysis of Si, Zr, and Y was performed by an energy-

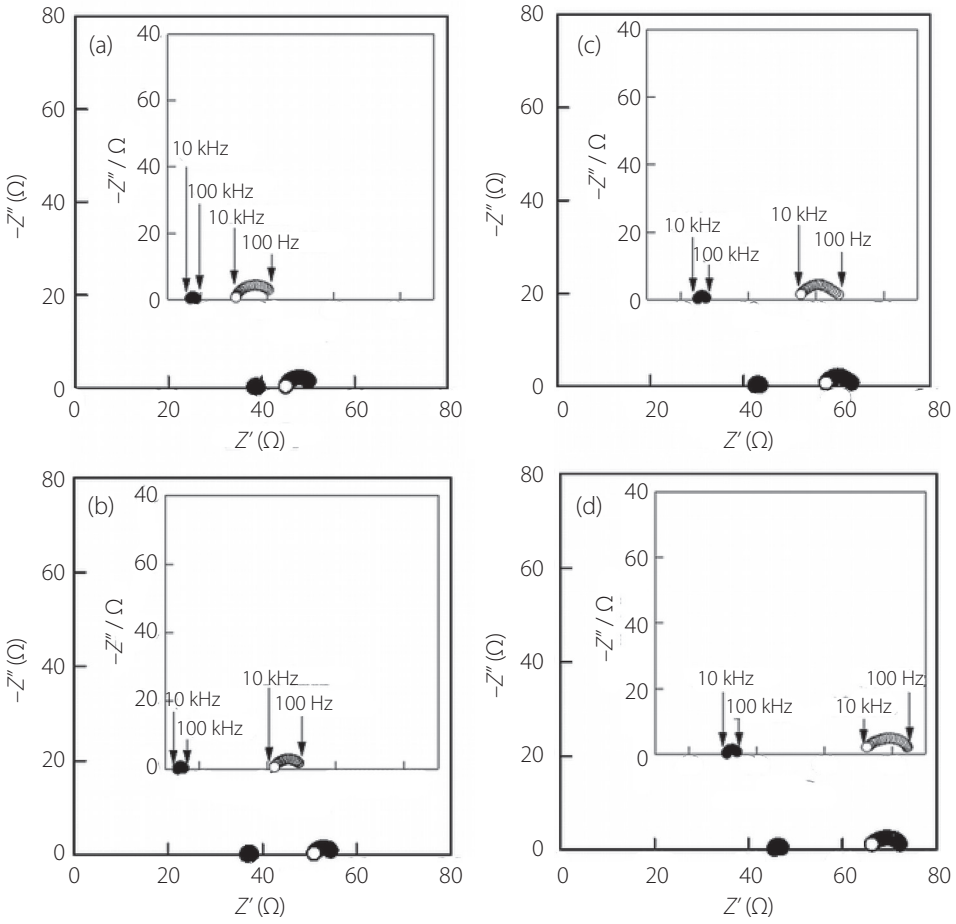


Figure 3: Nyquist plot before (filled circle) and after (open circle) the DC voltage load test of 8YSZ ($SiO_2$ contents: (a) < 40 ppm, (b) 550 ppm, (c) 1200 ppm, and (d) 2800 ppm) at 800 °C: The inset shows an enlarged view

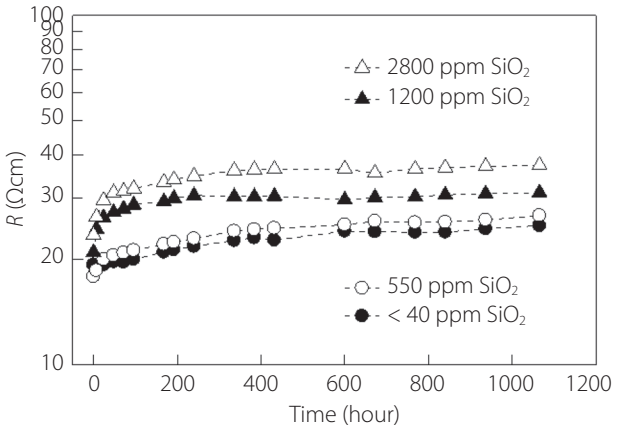


Figure 4: Relationship between elapsed time and DC resistance ($R_{dc}$) at 800 °C during the DC voltage load test

dispersive X-ray spectroscope, but specific elements were not concentrated and detected in the black spots. Before and after the test, there was no change in morphology, such as crystal grain size.

The XRD peaks observed in all samples were only those attributed to cubic $ZrO_2$, and no change was observed in the XRD patterns before and after the DC voltage load test as seen in Figure 7. This result is consistent with a previous report stating that the synchrotron XRD patterns of 8YSZ sintered at 1500 °C did not change after annealing at 800 °C for 2000 h in the atmosphere (Itoh, 2016).

## 4. Conclusion

The influence of $SiO_2$ (< 40, 550, 1200, and 2800 ppm) contained in 8YSZ ceramics that are used as solid electrolytes in SOFCs on the electrical characteristics was investigated using the DC voltage load test (in air, at 800 °C, for 1000 h, and under DC 1 V load). The following facts were clarified:

- As the $SiO_2$ content increased, the grain-boundary resistance of 8YSZ obtained by complex impedance analysis at 300 °C increased, while the bulk resistance remained constant. Therefore, $SiO_2$ is considered to be segregated at the grain-boundary.
- Although the DC resistance during the DC voltage load test increased immediately after the beginning of the test for all samples, it tended to stabilize as time elapsed. Ultimately, the DC resistance became almost constant after 600 h or more.
- The bulk resistance and the grain-boundary resistance

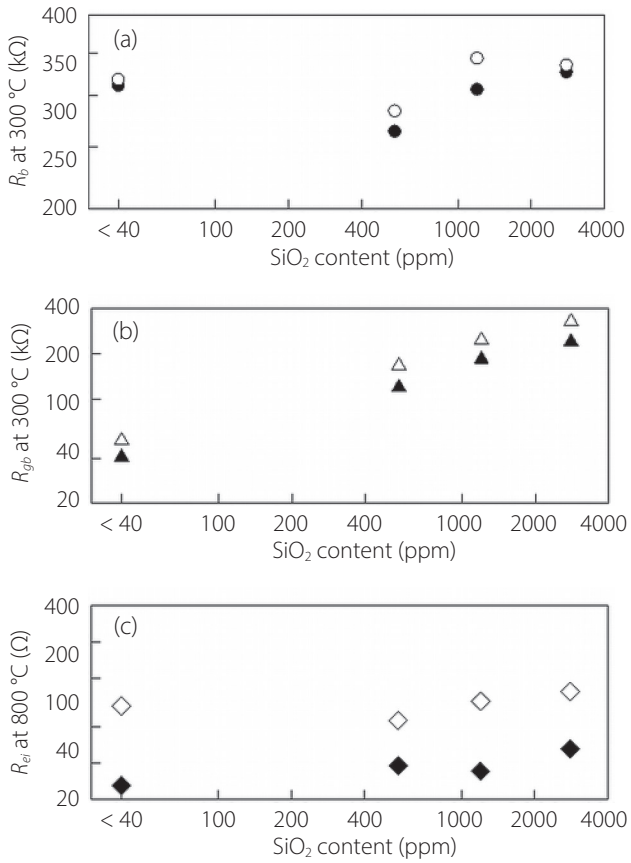


Figure 5: Relationship between content of $SiO_2$ in 8YSZ and each resistance ((a) bulk resistance ($R_b$) at 300 °C, (b) grain-boundary resistance ($R_{gb}$) at 300 °C, (c) electrode interface resistance ($R_{ei}$) at 800 °C before (filled mark) and after (open mark) the DC voltage load test)

obtained by complex impedance analysis at 300 °C after the DC voltage load test increased by 2-10 % and 23-28 %, respectively, compared with the respective initial values irrespective of the $SiO_2$ content.

- The arc originating from the electrode interface resistance was observed by complex impedance analysis at 800 °C and the resistance also increased after the DC voltage load test.

## Acknowledgement

We would like to thank Editage (www.editage.jp) for help with English language editing.

## References

Bouhamed, H. (2017). Improved structural stability and electrochemical performance of 8YSZ electrolyte by MxOy doping for low temperature solid oxide fuel cells (LT-SOFCs). *Materials Science & Engineering B*, Vol. 225, 182-188.

Ciacchi, F. T. and Badwal, S. P. S. (1991). The system $Y_2O_3$-$Sc_2O_3$-$ZrO_2$: Phase stability and ionic conductivity studies. *Journal of the European Ceramic Society*, Vol. 7, 197-206.

Cong, L., Hanying, L., Yuming, H., Shiyong, Z., Xiao, W., Tengfei, L., Xinghua, Z., and Xing, Y. (2020). Phase evolution and enhanced sinterability of cold sintered Fe2O3-doped 8YSZ. *Ceramics International*, Vol. 46, 14217-14223.

Hattori, M., Takeda, Y., Lee, J. H., Ohara, S., Mukai, K., Fukui, T., Takahashi, S., Sakaki, Y., and Nakanishi, A. (2004). Effect of annealing on the electrical conductivity of the $Y_2O_3$-$ZrO_2$ system. *Journal of Power Sources*, Vol. 131, 247-250.

Hughes, A. E. and Badwal, S. P. S. (1991). Impurity and yttrium

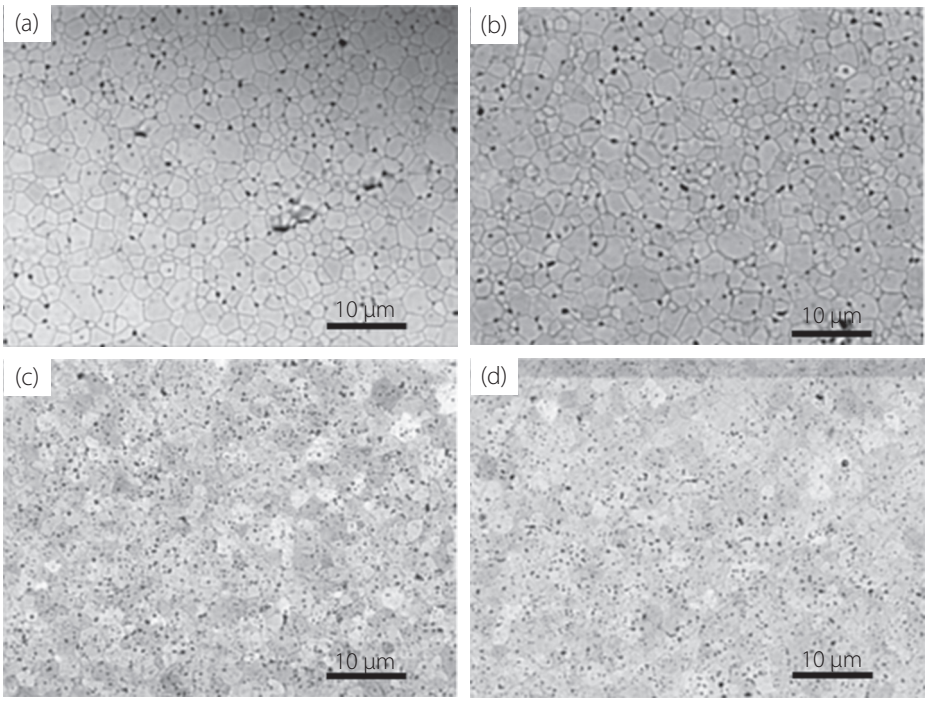


Figure 6: Reflected electron images of thermally etched surface of 8YSZ ($SiO_2$ contents: (a) and (b) < 40 ppm, and (c) and (d) 2800 ppm) before ((a) and (c)) and after ((b) and (d)) the DC voltage load test

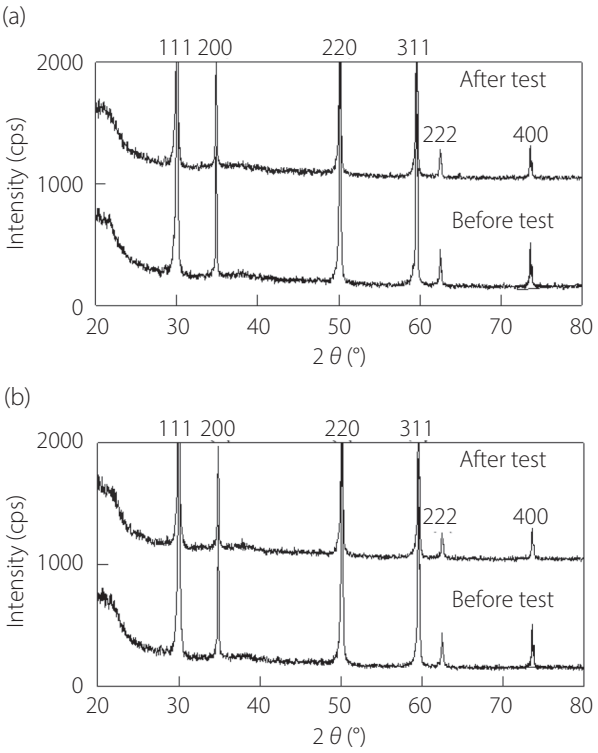


Figure 7: XRD patterns of grinded surface of 8YSZ ($SiO_2$ contents: (a) < 40 ppm and (b) 2800 ppm) before and after the DC voltage load test. Numbers represent miller index of cubic $ZrO_2$ reported in ICDD No. 27-997

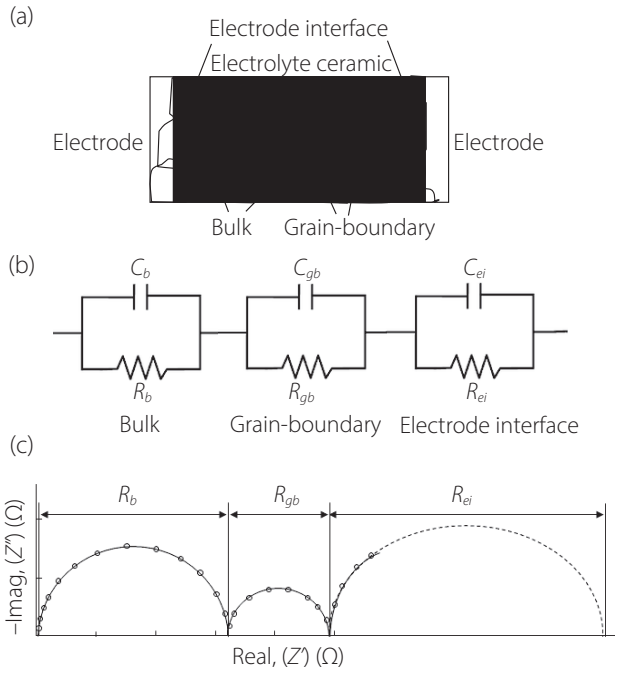


Figure 8: (a) Various components generated in the microstructure of electrolyte ceramic (ion conductor) and electrodes, (b) typical equivalent circuit, and (c) Nyquist plot example for the equivalent circuit

segregation in yttria-teragonal zironia. *Solid State Ionics*, Vol. 46, 265-274.

Itoh, T., Mori, M., Idemoto, Y., Imai, H., and Nakayama, M. (2016). Annealing effect on phase stability of doped zirconia using experimental and computational studies. *Solid State Ionics*, Vol. 297, 20-28.

Kwon, O. H. and Choi, G. M. (2006). Electrical conductivity of thick film YSZ. *Solid State Ionics*, Vol. 177, 3057-3062.

Samui, A. B., Patil, D. S., Prasad, C. D., and Gokhale, N. M. (2016). Synthesis of nanocrystalline 8YSZ powder for sintering SOFC material using green solvents and dendrimer route. *Advanced Powder Technology*, Vol. 27, 1879-1884.

Tikkanen, H., Suciu, C., Wærnhus, I., and Hoffmann, A. C. (2011). Dip-coating of 8YSZ nanopowder for SOFC applications. *Ceramics International*, Vol. 37, 2869-2877.

Yamamoto, O., Arati, Y., Takeda, Y., Imabishi, N., Mizutani, Y., Kawai, M., and Nakamura, Y. (1995). Electrical conductivity of stabilized zirconia with yttrebia and sacndia. *Solid State Ionics*, Vol. 79, 137-142.

## Appendix

As shown in Figure 8 (a), the electrolyte ceramic (ion conductor) is formed a collection of bulks (grains, microcrystals). The behavior of bulk, the behavior of grain-boundary, and the behavior of the interface with electrolyte-electrode are appear the Nyquist plot shown in Figure 8 (c). The typical equivalent circuit is shown in Figure 8 (b). There are bulk resistance ($R_b$), grain-boundary resistance ($R_{gb}$), and charge transfer resistance (electrode interface resistance, $R_{ei}$) as resistances that hinder ion conduction. When direct current (DC) is applied, the sum of these resistance components is the resistance ($R_{dc}$) of the entire electrolyte ceramic. ($R_{dc} = R_b + R_{gb} + R_{ei}$) When alternating current (AC) is applied, different frequency responses appear because the relaxation time of each behavior is different. In the equivalent circuit, the capacitance components are connected in parallel to each component, and the capacitances corresponding to each behavior are called bulk capacitance ($C_b$), grain-boundary capacitance ($C_{gb}$), and electric double layer capacitance (electrode interface capacitance, $C_{ei}$). The Nyquist plot example of this equivalent circuit is as shown in Figure 8 (c).

(Received: September 17, 2021; Accepted: November 11, 2021)